

Electronic Supplementary Information

High-quality WS₂ film formed on pristine ITO as Hole Transport Layer Film in high-efficiency Non-fullerene Solar Cells

Xiaojing Wang,^{‡a} Peng Liu,^{‡a} Boonkar Yap,^b Zhicai He,^{*a} Ruidong Xia^b and Wai-Yeung Wong^c

^[a] State Key Laboratory of Luminescent Materials and Devices, Institute of Polymer Optoelectronic Materials and Devices, South China University of Technology, Guangzhou, Guangdong, 510640, China.

*E-mail: zhicaihe@scut.edu.cn

^[b] The International School of Advanced Materials, School of Material Science and Engineering, South China University of Technology, Guangzhou, Guangdong, 510640, China.

^[c] Department of Applied Biology and Chemical Technology, The Hong Kong Polytechnic University (PolyU), Hung Hom, Hong Kong, 999077, China.

^[‡]These authors contributed equally to this work.

1. Supporting Tables

Table S1. The carrier mobility measurement in PM6: Y6 OSCs with different HTLs.

Device structure	u_h (cm ² V ⁻¹ s ⁻¹)	u_e (cm ² V ⁻¹ s ⁻¹)
ITO _{plasma} /WS ₂ /PM6:Y6/MoO ₃ /Ag	3.46×10 ⁻⁴	—
ITO/WS ₂ /PM6:Y6/MoO ₃ /Ag	1.97×10 ⁻³	—
ITO/PEDOT: PSS/PM6:Y6/MoO ₃ /Ag	8.02×10 ⁻⁴	—
ITO/ZnO/PM6:Y6/PFN-Br/Ag	—	8.89 × 10 ⁻⁴

Table S2. The carrier combination lifetime and carrier extraction time fitted from TPV and TPC curves.

Anode/HTL	τ (us) ^a	τ (us) ^b
ITO _{plasma} /WS ₂	1.03	0.74
ITO/WS ₂	3.95	0.65
ITO _{plasma} /PEDOT:PSS	3.56	0.64

^a carrier combination lifetime

^b carrier extraction time

Table S3. The calculation result of <N> values form UV-Vis spectroscopy.

Sampl e	Initial concentration (mg/mL)	Sonic processing time (h)	A-exction position (nm)	Thickness <N>
		6	622	3.51
WS ₂	6	9	617	1.95
		12	614	1.37

Note:The mean layer number of WS₂ nanosheets exfoliated in initial 6mg/mL solution with a range of sonic processing time from 6 to 12 h were estimated using the following equation:¹

$$\langle N \rangle = 6.35 \times 10^{-32} e^{\lambda_A(nm)/8.51}$$

2. Supporting Figures

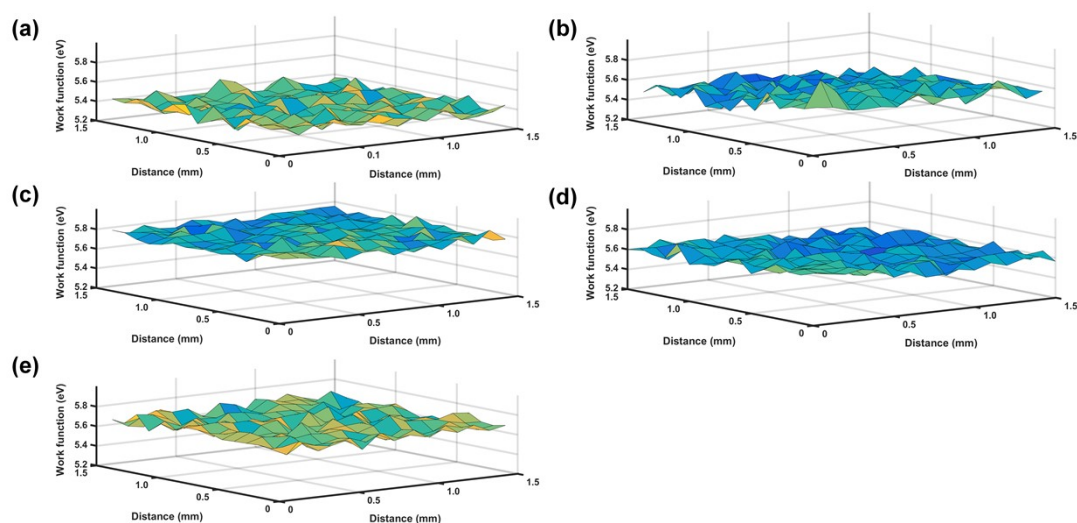


Figure S1. The scanning kelvin probe measurement (SKPM) of WS_2 films as HTLs preparing by different processing conditions. The initial concentration of WS_2 is 6 mg/mL, and (a), (b), (c) represents 6, 9, 12 h sonic processing time, respectively. The sonic processing time is 9 h, and (d), (e) represents 10 mg/mL, 14 mg/mL initial concentration of WS_2 , respectively.

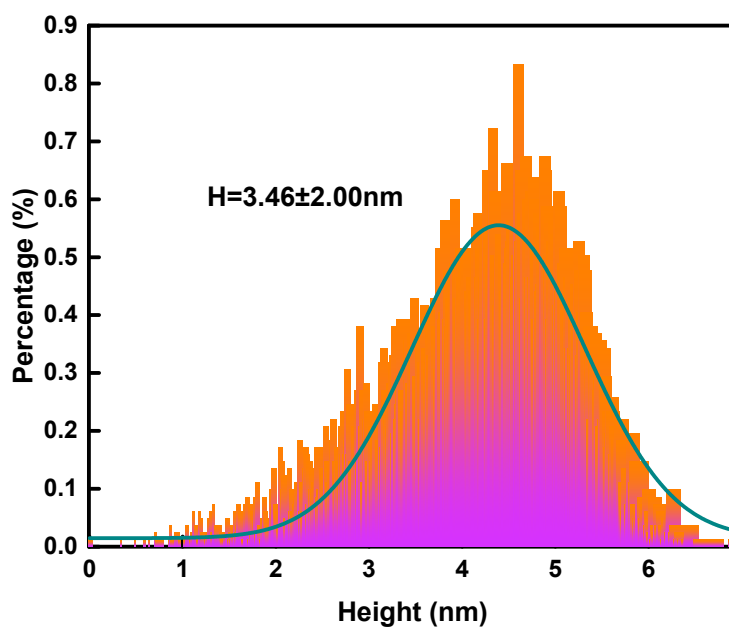


Figure S2. The percentage histogram of height of WS_2 nanosheet (Figure 6a), fitted by Gaussian distribution.

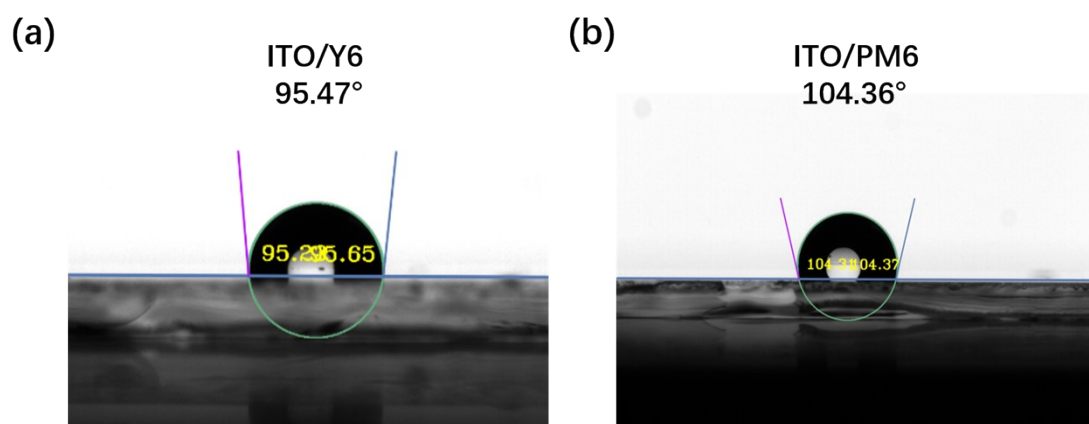


Figure S3. The water contact angle on the surface of ITO/ Y6 film (a) and ITO/PM6 film (b).

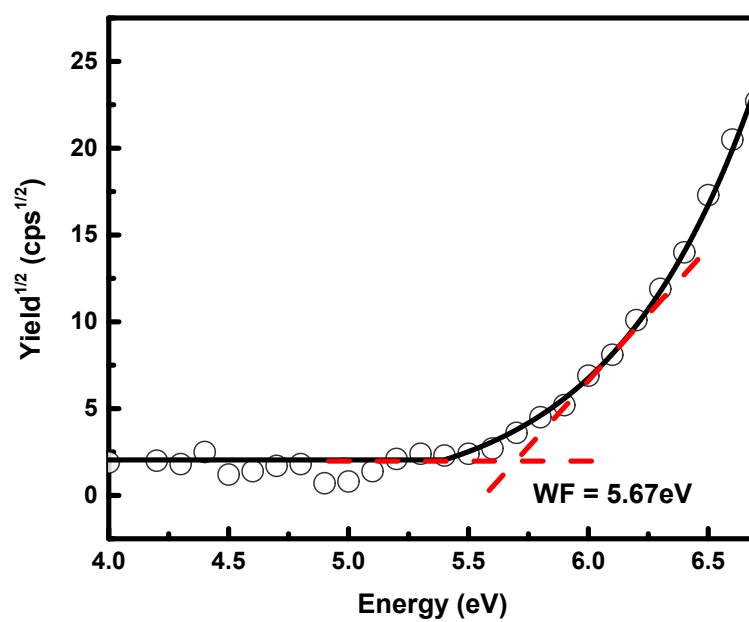


Figure S4. The ultraviolet photoelectron spectroscopy (UPS) measurement of WS₂ film.

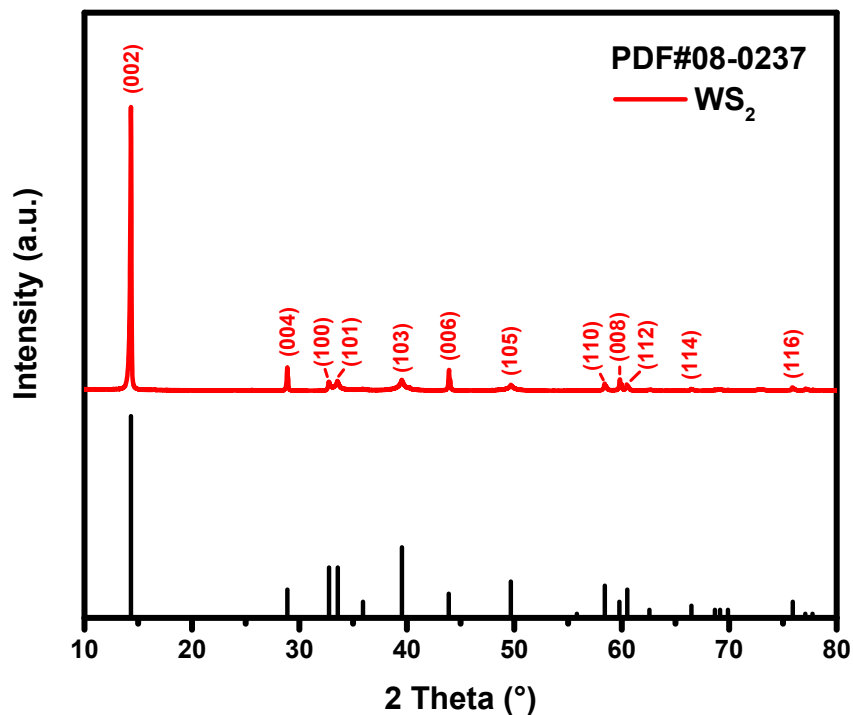


Figure S5. The X-ray diffraction (XRD) pattern of the WS₂ powder.

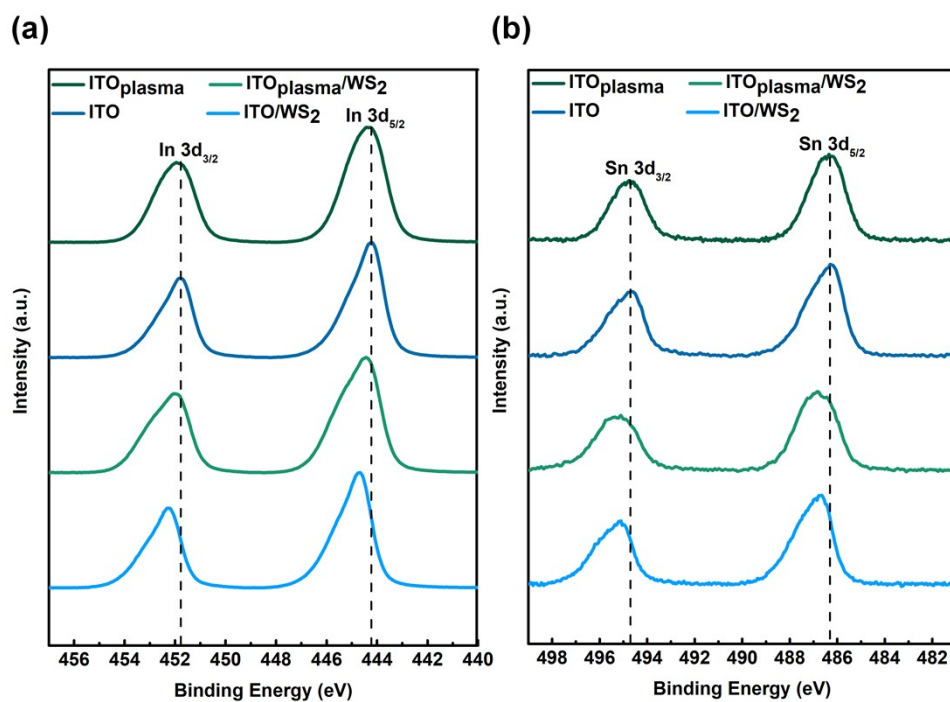


Figure S6. The XPS spectra of (a) In 3d, (b) Sn 3d of ITO nanoparticles.

Note: We have performed XPS test (shown in Figure S6) to elucidate the influence of the plasma treatment of ITO on the deposition of WS_2 . For the ITO nanoparticles, the binding energies (BEs) of a photoelectron in $In\ 3d_{5/2}$, $In\ 3d_{3/2}$, $Sn\ 3d_{5/2}$, and $Sn\ 3d_{3/2}$ are determined to be 444.1, 451.7, 486.3 and 494.7 eV, respectively.² This is consistent with our results shown in Figure S6. When WS_2 film is spin-coated on pristine ITO without plasma, the BEs of $In\ 3d_{5/2}$, $In\ 3d_{3/2}$, $Sn\ 3d_{5/2}$, and $Sn\ 3d_{3/2}$ shift upwards about 0.5eV, possibly caused by W or S bonding with Dangling bonds of In and Sn resulted from the oxygen vacancies in ITO.³ In the case of WS_2 film spin-coated on plasma-treated ITO, the BEs shift of $In\ 3d_{5/2}$ and $In\ 3d_{3/2}$ can be ignored, indicating less W or S bonds with In due to the disappear of Dangling bonds by plasma filling oxygen vacancies of ITO. Therefore, stronger chemisorption is formed between WS_2 and pristine ITO than plasma-treated ITO, thus influencing the deposition behavior of WS_2 .

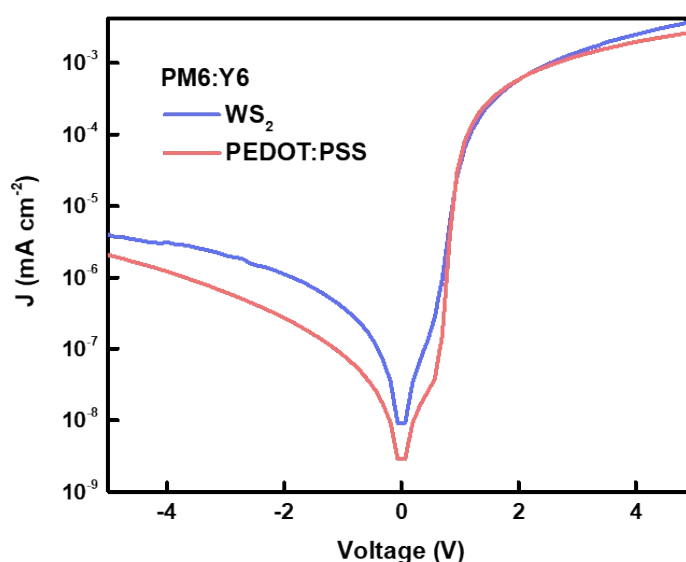


Figure S7. The dark J-V curves of the OSCs with WS_2 and PEDOT: PSS as HTLs.

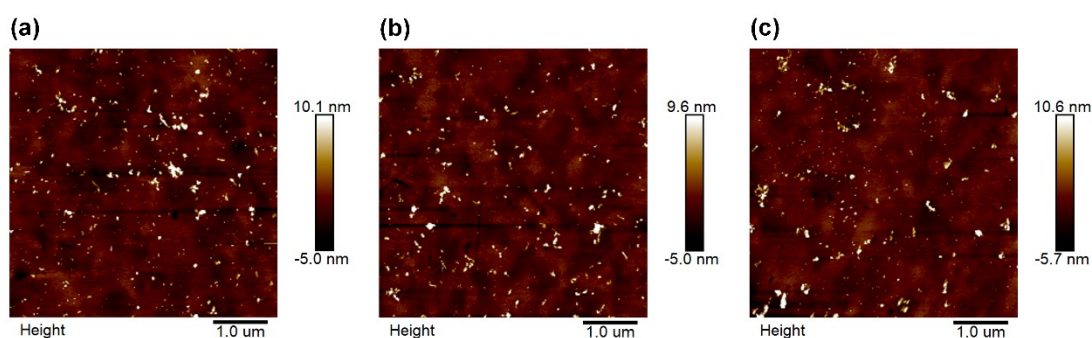


Figure S8. AFM images of WS_2 nanosheets exfoliated in 6mg/mL initial solution with 6h, 9h, 12h sonic processing time (a, b, c), respectively.

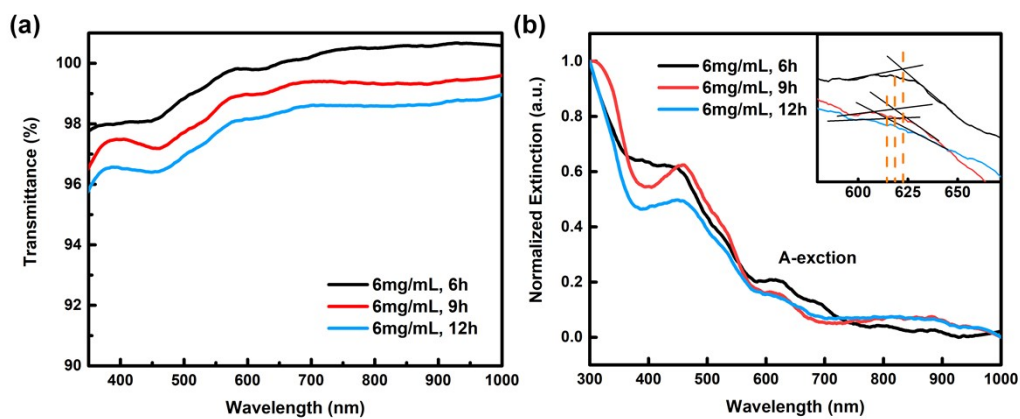


Figure S9. (a) Transmittance spectra of WS₂ nanosheets exfoliated in initial 6mg/mL solution with a range of sonic processing time from 6 to 12 h. (b) Optical extinction spectra of WS₂ nanosheets exfoliated in initial 6mg/mL solution with a range of sonic processing time from 6 to 12 h. The spectra normalized to the extinction value at 300 nm and the inset shows the magnified view of the A-exciton region.

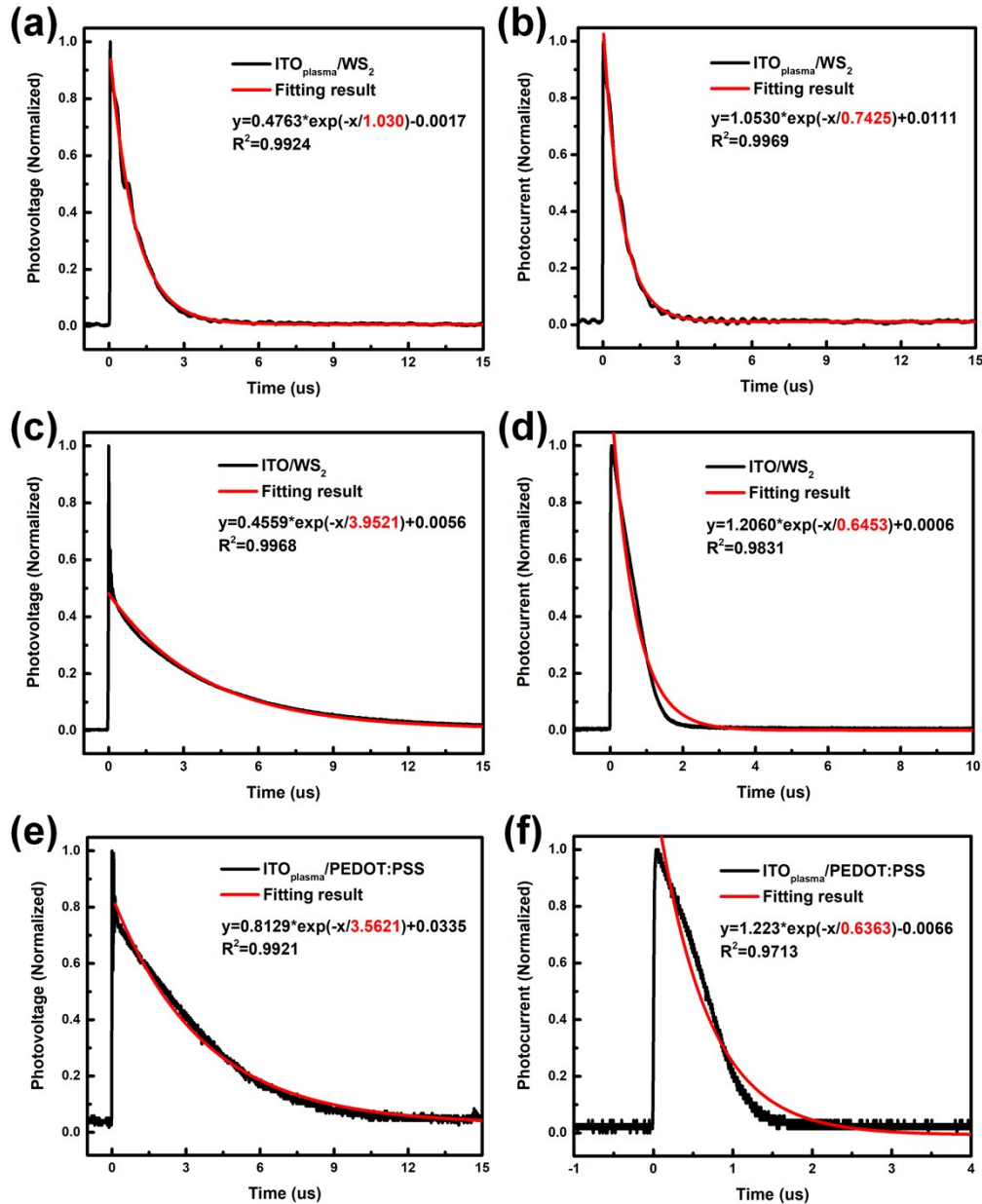


Figure S10. The measurement data (black lines) and fitting results (red lines) of TPV (a, c, e) and TPC (b, d, f) of devices based on three modified anodes: ITO_{plasma}/WS₂, ITO/WS₂, and ITO_{plasma}/PEDOT: PSS.

3. Supplementary Methods

Calculation methods of carrier combination lifetime and carrier extraction time from TPV and TPC:⁴

For the Transient Photovoltage (TPV) measurements, a weakened 620 nm laser pulse with a pulse width of 120 fs was used as the light source, which makes the device produce a small transient voltage on the basis of the steady voltage. The

measuring equipment was linked to a Tektronix TDS 3052C digitizing oscilloscope in the open-circuit conditions. After filtering the DC signal, we can get the transient photovoltage signal, which is a single exponential decay curve. The decay life can be obtained by exponential fitting with the exponential decay formula as following:

$$V = V_0 \exp\left(-\frac{t}{\tau}\right)$$

Also, we can obtain the transient photocurrent (TPC) signal and the carrier extraction time can be obtained by exponential fitting with the exponential decay formula as following:

$$I(t) = I_0 \exp\left(-\frac{t}{\tau}\right)$$

Calculation methods of carrier mobility:

The carrier mobility of the hole-only devices (electron-only devices) was extracted by fitting the voltage via the space charge limited current (SCLC) Mott-Gurney equation as follows:

$$J = 9\epsilon_r\epsilon_0\mu V^2/8d^3$$

where ϵ_r is the relative dielectric constant, ϵ_0 is the permittivity of vacuum, d is the thickness of the active layer, μ_e (μ_p) is the electron (hole) mobility.⁵

Contact angle measurements:

The contact angle tests were performed on DSA-x plus optical contact angle analyzer. The surface energy of the materials was characterized and calculated by the contact angles of the two probe liquids with the Owens and Wendt equation:⁶

$$(1 + \cos \theta)\gamma_{pl} = 2(\gamma_s^d \gamma_{pl}^d)^{1/2} + 2(\gamma_s^p \gamma_{pl}^p)^{1/2}$$

where γ_s and γ_{pl} are the surface energy of the sample and the probe liquid,

respectively. The superscripts d and p refer to the dispersion and polar components of the surface energy, respectively.

References

- ¹ C. Backes, B. M. Szydłowska, A. Harvey, S. Yuan, V. Vega-Mayoral, B. R. Davies, P.-I. Zhao, D. Hanlon, E. J. G. Santos, M. I. Katsnelson, W. J. Blau, C. Gadermaier and J. N. Coleman, *ACS Nano*, 2016, **10**, 1589-1601.
- ² S.-N. Kim, S.-B. Kim and H.-C. Choi, *Bulletin of the Korean Chemical Society*, 2012, **33**, 194-198.
- ³ M. Timpel, H. Li, M. V. Nardi, B. Wegner, J. Frisch, P. J. Hotchkiss, S. R. Marder, S. Barlow, J. L. Brédas and N. Koch, *Advanced Functional Materials* 2018, **28**, 1704438.
- ⁴ C.G. Shuttle, B. O'Regan, A.M. Ballantyne, J. Nelson, D.D.C. Bradley, J.D. Mello, J. R. Durrant, *Appl. Phys. Lett.*, 2008, **92**, 093311.
- ⁵ I. Zonno, A. Martinez-Otero, J.-C. Hebig and T. Kirchartz, *Physical Review Applied*, 2017, **7**, 034018.
- ⁶ X. Liu, C.H. Zhang, C. H. Duan, M. M. Li, Z. C. Hu, J. Wang, F. Liu, N. Li, C. J. Brabec, R. A. J. Janssen, G. C. Bazan, F. Huang, and Y. Cao, *J. Am. Chem. Soc.*, 2018, **140**, 8934–8943.